



Enhancement of sonochemical production of hydroxyl radicals from pulsed cylindrically converging ultrasound waves

Cherie C.Y. Wong^a, Jason L. Raymond^a, Lillian N. Usadi^a, Zhiyuan Zong^a,
Stephanie C. Walton^a, Adam C. Sedgwick^b, James Kwan^{a,*}

^a Department of Engineering Science, Parks Road, Oxford OX1 3PJ, UK

^b Department of Chemistry, Chemistry Research Laboratory, University of Oxford, Mansfield Road, OX1 3TA, UK

ARTICLE INFO

Keywords:

Sonochemistry
Ultrasound
Cavitation
Reactive Oxygen Species
Dosimetry

ABSTRACT

Sonochemistry is the use of ultrasound to generate highly reactive radical species through the inertial collapse of a gas/vapour cavity and is a green alternative for hydrogen production, wastewater treatment, and chemical synthesis and modifications. Yet, current sonochemical reactors often are limited by their design, resulting in low efficacy and yields with slow reaction kinetics. Here, we constructed a novel sonochemical reactor design that creates cylindrically converging ultrasound waves to create an intense localised region of high acoustic pressure amplitudes (15 MPa_{rms}) capable of spontaneously nucleating cavitation. Using a novel dosimetry technique, we determined the effect of acoustic parameters on the yield of hydroxyl radicals (HO•), HO• production rate, and ultimately the sonochemical efficiency (SE) of our reactor. Our reactor design had a significantly higher HO• production rate and SE compared to other conventional reactors and across literature.

1. Introduction

Sonochemistry is regarded as a promising green chemical pathway for many chemical products, including reactive oxygen species [1], hydrogen gas [2], and high-valued chemicals [3,4]. To achieve these reactions, sound waves (ultrasound) in the range of 16 to 3000 kHz are used to nucleate and subsequently volumetrically oscillate gas-vapour bubbles in a liquid (acoustic cavitation) [5]. With sufficient acoustic power, these bubbles undergo volumetric changes governed largely by the inertia of the liquid that may result in an inertial collapse. As bubbles collapse, the inertial confinement of trapped gas and vapour is a quasi-adiabatic process that increases the temperature and pressure to greater than 5000 K and 1000 bars, respectively [6]. At these extreme conditions, the gas and vapour undergo pyrolysis to form highly reactive free radicals. For example, inertial collapse of bubbles in water will partially split the water molecules into both hydrogen radicals (H•) and hydroxyl radicals (HO•) (Eq. 1). Though H• is short lived, the HO• may diffuse into the bulk liquid phase and initiate other chemical reactions. This reactive chemical environment created by acoustic cavitation has demonstrated utility in applications such as drug delivery [7], chemical synthesis [8], and pollutants degradation [9].



Considering that acoustic cavitation underpins sonochemistry and the acoustic field nucleates cavitation, it follows that controlling the acoustic field in the liquid is crucial for optimal sonochemistry. Thus, much thought must be given to both the operating conditions (frequency, pressure amplitude, duty cycle, etc.) and the design of the sonochemical reactor, which broadly consists of an ultrasound transducer, a reaction vessel, and a coupling medium to connect the sound source to the reactants. Often, this coupling medium is also the solvent containing the reactants. Common ultrasonic reactor designs reported in the literature include ultrasonic bath reactors, immersed horn reactors, and cup-horn reactors. We encourage readers to refer to an in-depth critical review of different types of ultrasonic reactors by Meroni *et al.* [10]. Yet, most of the reactor designs are limited by dispersed acoustic energy and therefore often require continuous and substantial acoustic drive power for long durations to achieve meaningful yields. Moreover, the design of these reactors makes it difficult to deliver consistent acoustic energy to a reaction volume, resulting in difficulties in reproducing sonochemical reactions.

In this article, we present a novel sonochemical cylindrical reactor design (SonoCYL) that guides acoustic waves to a reactor vessel. These converging waves cause intense localised acoustic pressure fields. The

* Corresponding author.

E-mail address: james.kwan@eng.ox.ac.uk (J. Kwan).

<https://doi.org/10.1016/j.ultsonch.2023.106559>

Received 2 June 2023; Received in revised form 8 August 2023; Accepted 14 August 2023

Available online 18 August 2023

1350-4177/© 2023 The Author(s). Published by Elsevier B.V. This is an open access article under the CC BY-NC-ND license (<http://creativecommons.org/licenses/by-nc-nd/4.0/>).

novel reactor design is analogous to a high intensity focused ultrasound (HIFU) transducer. Yet most HIFU transducers use spherical lensing to create a point-like focus. In contrast, the cylindrical acoustic field from SonoCYL was produced by reflecting a spreading wave to create a converging wave. In this focused acoustic field, we observed spontaneous nucleation of cavitation. To measure a chemical effect resulting from this cavitation, we utilised a highly sensitive and HO^\bullet selective molecular fluorescence probe to dosimetrically quantify the yield of HO^\bullet generated in PBS at various operating conditions for SonoCYL. Furthermore, we determined that SonoCYL has a higher HO^\bullet production rate and sonochemical efficiency (SE) compared to conventional sonochemical reactors. Ultimately, we hope that this design strategy may lead to scalable industrially relevant sonochemical reactors.

2. Materials and methods

2.1. Materials

The chemicals used are as follows: ethylenediaminetetraacetic acid (ACS reagent, 99.4–100.6%, powder, Merck), hydrogen peroxide (30 % (w/w) in water, Merck), iron(II) chloride tetrahydrate (ReagentPlus, 98%, Merck), *n,n*-Dimethylformamide (DMF, anhydrous, 99.8%, Merck), and phosphate buffered saline (PBS, Tablet, Merck). All chemicals were used without further processing unless otherwise stated.

De-ionised filtered Type 1 water (DI water) was obtained from a water purification system (Millipore Direct Q5-UV). Degassed DI water was prepared using a bespoke degas unit. The unit consisted of a membrane contractor (3 M Liqui-Cel™ G541), a water pump (Flojet LFP, 24 V RLFP222202D), and a vacuum pump (Welch MPC 090 E, type 412021). DI water was considered degassed until the oxygen concentration reached less than 20%, which was measured by Duo pH/Ion/DO meter SG98, Mettler Toledo.

Austenitic stainless steel (316 alloy, Taybroh Alloys) was used for the construction of SonoCYL. The ultrasound transducer used in the reactor was a cylindrical tube piezoelectric ceramic (Type I lead zirconate titanate (PZT), APC International, Ltd) with a dimension of 38 mm outer diameter, 34 mm inner diameter and 25 mm length. All materials were used without further processing unless otherwise stated. All sonochemical reactions were performed in 5 mL polypropylene (PPE) test tubes (Scientific Laboratory Supplies).

2.2. Reactor design and experimental set-up

2.2.1. Reactor design

Fig. 1 shows a schematic and a picture of the reactor. The manufacturers of the parts are listed in Section 2.1. The sonochemical cylindrical reactor (SonoCYL) was constructed of stainless steel and was designed to have two conical reflectors with a 45° bevel. The reflectors immediately adjacent to the top and bottom plate to reflect the acoustic wave, where each reflection changes the direction of propagation by 90° . These 45° reflectors were spaced approximately 30 mm apart with a spacer (cylindrical stainless steel tube) and capped with a top and bottom plate. The top plate consisted of an opening for placing a vessel for reagents and samples (5 mL PPE test tube). Centred on the 16 cm diameter bottom plate was the tube ultrasound transducer, which consisted of a cylindrical tube PZT mounted onto a Delrin plastic holder to ensure central alignment with the bottomed plate.

Prior to any acoustic experiments, the SonoCYL was slowly filled with degassed DI water to couple the transducer to the reaction vessel and minimise the chances of unwanted acoustic cavitation from dissolved bubbles in the coupling medium. During any acoustic measurements and sonochemical reactions, the cylindrical tube transducer at the bottom of the reactor was operated at the measured resonant frequency of 1 MHz. The transducer had an impedance of ~ 50 Ohm when submerged in the degassed DI water, omitting the need for an impedance matching network.

Fig. 1(a) shows the schematic of the SonoCYL design. Driving the transducer in thickness mode emitted a radially spreading acoustic pulse. The radially spreading pulse was reflected by the bottom 45° reflector, then transmitted through the spacer, and finally reflected again by the top 45° reflector, the acoustic wave was effectively rotated 180° , creating a cylindrically converging wave with a focus along the longitudinal axis of the reactor vessel.

2.2.2. Experimental set-up

Fig. 2 shows the experimental set-up for acoustic pressure characterisation and sonochemical reactions. To drive the transducer, a sine wave signal was generated from a function generator (Keysight Waveform Generator, 33400A). The signal from the function generator was first attenuated using a -20 dB attenuator before being amplified by a 55 dB radio-frequency (RF) amplifier (Electronics & Innovation 1040L RF Amplifier) and transmitted to the ultrasound transducer. In line with the high-voltage signal was a current probe and voltage probe, which were connected to an oscilloscope (LeCroy, LT264). The static

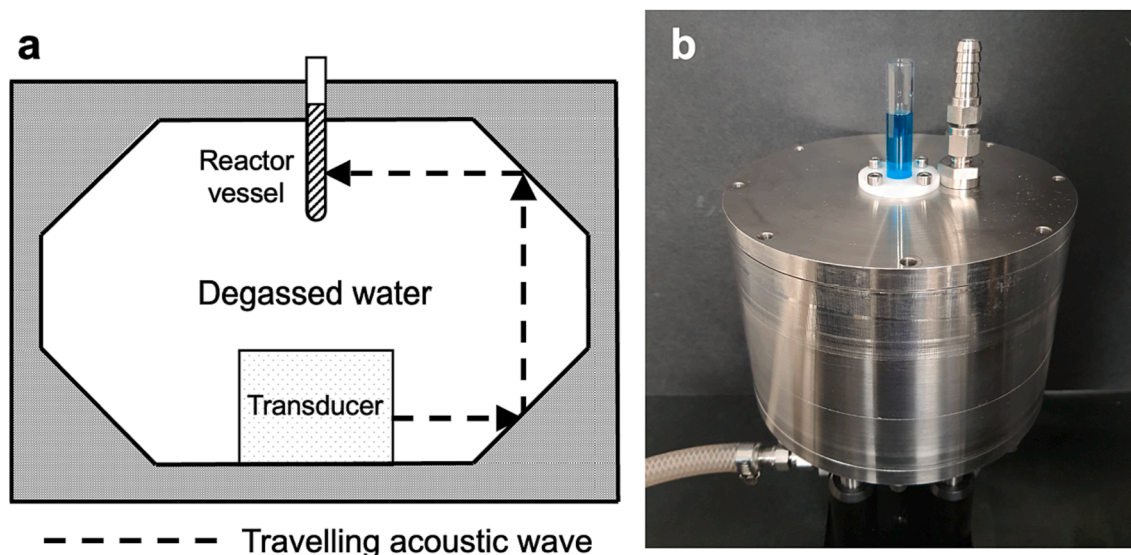


Fig. 1. (a) Schematic of the SonoCYL design. (b) Picture of the SonoCYL. The height of the cylindrical reactor is 11 cm with a diameter of 16 cm.

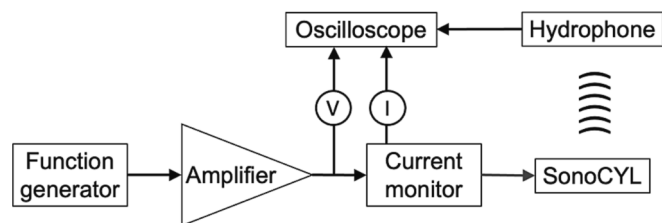


Fig. 2. Schematic experimental set-up for the acoustic pressure characterisation and sonochemistry. Note that for sonochemical reactions, the hydrophone was removed.

capacitance and resonance of the PZT were measured using an inductance, capacitance, and resistance (LCR) meter (BK879B, BK Precision) and an impedance analyzer (Digilent Analog Discovery Impedance Analyzer and Digilent Analog discovery 2), respectively.

2.3. Acoustic pressure characterisation and sonochemical reactions

2.3.1. Acoustic field measurements

A needle hydrophone (Precision Acoustics, SN 3222) with a diameter of 0.2 mm was used to measure the acoustic pressure in the reaction vessel. For pressure field measurements, the hydrophone was placed on a 3D positioning system (3-Stepping Motor Controller, Velmex VXM) operated using a custom MATLAB script. The hydrophone was connected to an oscilloscope (LeCroy, LT264) to record hydrophone signals and determine maximum, minimum, peak-to-peak amplitudes, and phase angle. The input voltage, current (Pearson model 6027 1.0 V/A), and phase were also recorded by the oscilloscope to calculate the input electrical power to the transducer (Section 2.4 – Input electrical power calculation). A point scan relating drive voltage and power to acoustic pressure amplitude was measured at the focal point. For the acoustic measurement with the needle hydrophone, the number of cycles and the burst period were 50 and 10 ms, respectively. All reported acoustic pressure values were expressed as peak-to-peak pressure.

2.3.2. Acoustic waveform measurement

For the acoustic waveform measurement, a piezoelectric pin hydrophone (Dynasen, CA-1136) with a diameter of 0.093 in. was placed at the focal point in the reaction vessel. The hydrophone was connected to an oscilloscope (LeCroy, 334A) to record the acoustic waveform.

2.3.3. Sonochemical reactions

For driving sonochemical reactions with SonoCYL, the hydrophone was removed. The operating parameters for the sonochemical reactions are described in SI Section 1.

2.4. Sonochemical production of HO• and sonochemical efficiency (SE) determination

2.4.1. Reaction solution preparation

A stock phosphate buffer saline (PBS) was prepared by dissolving one PBS tablet into 200 mL of deionised water (pH 7.4 at 25 °C). The Resorufin-DHB (Res-DHB) compound was synthesised by the schematics (SI Scheme S2.1 and S2.2) according to a recent publication [11]. HO• dosimetry is conventionally conducted by Weissler reaction, Fricke reaction, and terephthalic acid (TA) assay. However, these dosimetry methods suffer from limitations including low accuracy and selectivity for HO• and temperature sensitivity. Therefore, here we conducted the HO• dosimetry using Res-DHB, a sensitive, temperature independent, and highly selective fluorescent probe. Res-DHB was pre-dissolved in DMF (5 mM) and added to PBS to make a 3 mL reaction solution with Res-DHB concentration at 5 μM. Before every sonochemical reaction, the reaction vessel was saturated with dissolved gas by vigorously shaking every two minutes. All reactions were performed at ambient

temperature and pressure.

2.4.2. Fluorescence measurements

A fluorometer (Perkin Elmer LS 55, $\lambda_{\text{excitation}} = 500 \text{ nm}$, $\lambda_{\text{emission}} = 585 \text{ nm}$, slit widths: excitation = 10 nm and emission = 3.5 nm) was used to detect the fluorescence from resorufin (Res). From the fluorescence spectrometer of Res, the HO• yield was quantified using a calibration curve of the fluorescent emission intensity vs the HO• concentrations. An example of the fluorescence spectrometry of the SonoCYL experiment using Res-DHB is shown on SI Figure S3.

2.4.3. Sonochemical efficiency (SE)

The sonochemical efficiency (SE) was determined from the correlation between the measured concentration of HO• and the energy (Eq. 2) used by the reactor.

$$E = (P)(t)(DC) \quad (2)$$

where E is the energy used for the sonochemical reaction, P is the drive power, t is the reaction time, and DC is the duty cycle (calculation of duty cycle is in SI Section 4).

2.4.4. Input power calculation

The input electrical power was calculated from the input voltage, current, and phase transmitted to the SonoCYL using Eq. 3,

$$P = I_{\text{rms}} V_{\text{rms}} \cos(\theta) \quad (3)$$

where P is the average power, I_{rms} is the root mean square (RMS) current, and V_{rms} is the RMS voltage. An alternative method to determine power from the acoustic transducer was determined by measuring the temperature change in the reaction vessel. To measure the temperature, we inserted a thermocouple (N-type) into the sample solution and used a thermometer to measure the temperature reading (Fluke 54 II B). The derivation of the heat transfer equations was used to fit the temperature data are described in SI Section 5.

2.5. Conventional sonochemical reactor

Three conventional sonochemical reactors were used in this study. They were an ultrasonic bath reactor (35 kHz, Bandelin Electronic Ultrasonic Bath RK 100) (SI Figure S6 (a)), an immersed horn reactor (40 kHz, Sonic Systems 021940A) (SI Figure S6 (b)), and a cup-horn reactor (583 kHz, Meinhardt Ultrasonics, E/805/T/solo) (SI Figure S6 (c)).

3. Results and discussion

3.1. Acoustic characterisation

Fig. 3 shows the spatial distribution of the acoustic pressure amplitude across two planes. For (a), the bottom of the top plate was defined as 0 mm in the z-axis. For (b), the position of peak acoustic pressure amplitude was defined as 0 mm in the x- and y-axis. The full-width half maximum (FWHM) for the x- and y-axis was ~ 0.5 mm and for the z-axis was ~ 5.9 mm (see SI Section 7). Based on these measurements, the acoustic focal volume was calculated to be ~1.16 μL. These measurements agreed with our expectations; the measured x- and y-axis FWHM was similar to the FWHM of the primary peak of the cylindrical Bessel function of the first kind (~0.7 mm assuming that the speed of sound of water is 1.481 mm/μs at 20 °C), suggesting that the converging waves constructively interfere at the centre of the reaction vessel. It is important to note here that the measurements were slightly off centre due to the space limitations to fit the hydrophone inside the reaction vessel.

In addition to the acoustic pressure distribution, we measured the range of pressure amplitudes achievable by the transducer since acoustic cavitation is in part governed by the acoustic pressure amplitude. Hydrophone measurements of the acoustic pressure amplitude at the

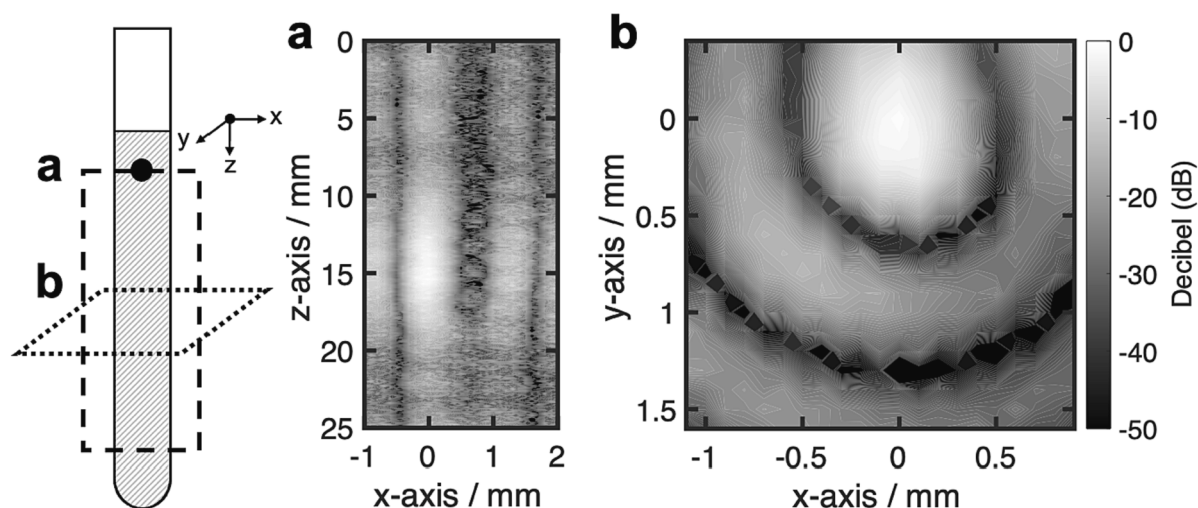


Fig. 3. (a) xz- and (b) xy- pressure scan in the reaction vessel.

spatial peak for different input electrical powers (SI Figure S8) were conducted at low drive powers to avoid damaging the hydrophone. Higher acoustic pressure amplitudes were then estimated by extrapolation from linear fit on SI Figure S8 (a). Thus, the maximum pressure amplitude achievable was estimated to be 15 MPa_{rpk}. However, the extrapolated acoustic pressure amplitudes outside the measured values may not be accurate due to the wave becoming increasingly non-linear with increasing power.

3.2. Res-DHB dosimetry for hydroxyl radicals

Chemical probes are commonly used to quantify HO• yield [12]. Conventionally, HO• dosimetry is performed by Weissler reaction, Fricke reaction, and terephthalic acid (TA) assay. However, the former two dosimetry methods assume HO• goes through specific reaction pathways to form H₂O₂ without any side reactions and the probes detect the concentration of H₂O₂. Yet, side reactions are present in practice, leading to inaccurate values of HO• yield [12,13]. Furthermore, Γ/Γ_3 equilibrium constant is temperature dependent in Weissler reaction [13,14]. Sonochemical reactors generate heat at different rates, hence shifting the Γ/Γ_3 equilibrium constant to different values. This suggested that the concentration of HO• may not be measured accurately using Weissler reaction in reactors that have large temperature changes [13]. On the other hand, even though TA assay is selective to HO• by reacting with the radicals via an arene hydroxylation reaction mechanism, its solubility is low in aqueous media and is highly pH sensitive [15]. The TA intermediate can also react with oxygen in air and undergo double OH-radical-induced hydroxylation to form side products [12,16]. Thus, TA assays are sensitive to the specific setup, making comparisons between literature difficult. Moreover, the three dosimetry assays require the chemical concentration in the range of milli-molar, which is not ideal in the detection of very low concentrations of HO• [12]. Here, we quantified the HO• yield by chemical dosimetry with resorufin-DHB (Res-DHB), a highly sensitive, temperature independent, and selective probe for HO• [11]. Similar to TA, Res-DHB proceeds with HO• via an arene hydroxylation reaction mechanism, which is selective to HO•.

Other radicals produced from inertial cavitation do not have this capability.

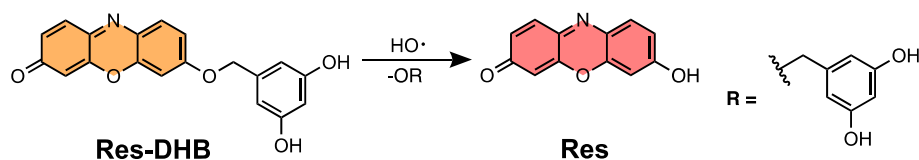
The reaction scheme of Res-DHB with HO• is illustrated on Scheme 1. A low concentration of Res-DHB was present in the solution, and as a non-stoichiometric amount of HO• was required to release Res and achieve a fluorescent response (SI Section 9 – Calibration curve and Fenton chemistry). This dose response curve was used to correlate HO• to measured fluorescence intensity and thus determine the HO• yield resulting from the sonochemical reaction.

During the preparation of the Res-DHB samples, we used PBS to maintain the pH of the reactants throughout the reaction. Res-DHB was shown to be stable in PBS and temperature insensitive at 60 °C, which is below the temperature rise under the ultrasonic irradiation with SonoCYL at the maximum power output (SI Figure S10) [11]. Before every sonochemical reaction, the reaction vessel was saturated with gas (i.e., reached the maximum capacity of dissolved gas) by vigorously shaking every two minutes to maximise the chances of inertial cavitation during the sonochemical reaction. The resulting fluorescent sample was measured to determine the amount of HO• in the all the sonochemical reactions.

3.3. Optimal operational parameters for SonoCYL

3.3.1. Dependence on acoustic pressure

Fig. 4 shows the concentration of HO• yield resulting from different acoustic pressure amplitudes. There was no observable presence of HO• for reactions at pressure amplitudes below 7.5 MPa_{rpk}. At 10.1 MPa_{rpk}, HO• were detected. This apparent threshold for HO• detection suggested there was a cavitation threshold between 7.5 MPa_{rpk} and 10.1 MPa_{rpk}, which confirms that acoustic inertial cavitation was the source for HO• and agrees with previous research [17]. Higher acoustic pressure amplitudes likely led to the nucleation of a larger population of bubbles that underwent inertial collapse and or forced bubbles to grow to a larger maximum radius just before the moment of implosion. Larger bubble radii before implosion generally increases the maximum temperature within the bubble [18]. Thus, both more nucleation sites and



Scheme 1. Reaction of Res-DHB with HO• yielding fluorescent Res probe. Res-DHB is orange in colour and Res is pink in colour. Res (λ_{ex} = 500 nm; λ_{em} = 585 nm).

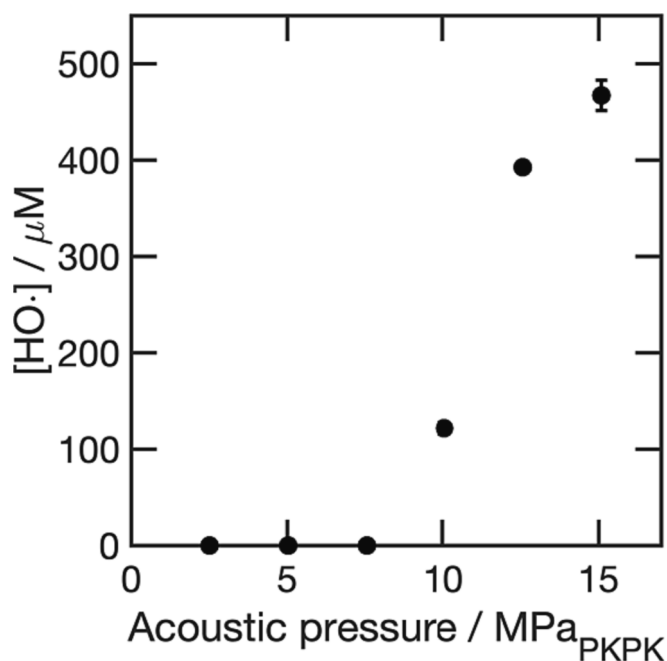


Fig. 4. The HO• concentration from the Res-DHB reaction at different acoustic pressure. Each value is the average of three trials and the error bars indicate the standard deviation.

larger bubble radii likely contributed to the increase in radicals produced in the reaction.

Cavitation thresholds in water are dependent on many factors and may range from 0.3 MPa to more than 12 MPa. We estimated a cavitation threshold between 7.5 MPa and 10.1 MPa at 1 MHz, which is higher than some literature values (0.3 to 0.4 MPa at 1 MHz) [19–21]. But our values do correspond to others [22–24]. This discrepancy may be due to inherent differences in the sources of ultrasound used and the operating conditions. The reported cavitation thresholds between 0.3 and 0.4 MPa at 1 MHz were measured in a standing wave field from a plate transducer likely operated in a continuous wave mode. However, SonoCYL delivers pulsed focused ultrasound and may be better compared to high intensity focused ultrasound (HIFU). Previous work determining cavitation thresholds in water using 1.1 MHz HIFU transducers reported that 5 MPa peak rarefactional pressure amplitude was not able to nucleate cavitation [22]. Other work indicated that cavitation thresholds of ~12 MPa peak rarefactional pressure amplitude were required to achieve cavitation ~50% of the time [24]. In addition, Lafon *et al.* has showed a 10 MPa acoustic pressure cavitation threshold measured with hydroxyl radical dosimetry [23]. This threshold was around twice higher than thresholds under continuous sonication.

3.3.2. Dependence on number of acoustic cycles

Sonochemical reactions are typically conducted using continuous wave (CW) ultrasound. Yet, pulsed ultrasound enhances sonochemical reactions though pulse lengths often exceed 10^5 cycles at moderate ($\geq 10\%$) duty cycles (DC) [25–28]. Thus, we measured the yield of HO• for different acoustic cycles (*i.e.*, burst length) at a fixed 9% DC (Fig. 5) to ensure that the energy input at a fixed reaction time remained the same across the different exposure conditions. Furthermore, this low DC prevented excessive heating and allowed any nucleated bubbles to dissolve into the liquid again after the burst ends.

We observed that 100 acoustic cycles produced the largest yield of HO•. It is noted that the concentration of hydroxyl radicals was higher at 10^4 cycles than 10^3 cycles. Yet, the difference between the two concentrations was merely less than 10%. Both data points were notably lower than the concentration of hydroxyl radicals at 100 cycles.

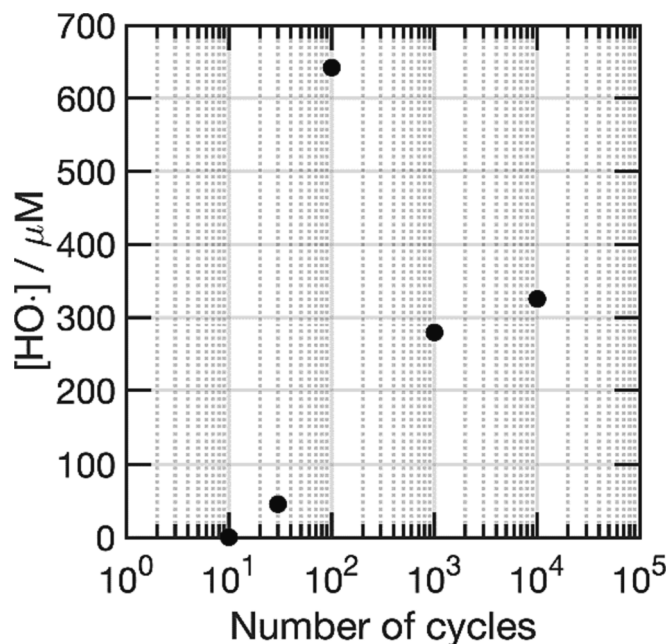


Fig. 5. The HO• concentration from the Res-DHB reaction at different number of cycles. Each value is the average of three trials and the error bars (overlapped with the markers) indicate the standard deviation.

Consider before and after the optimum number of cycles: below 100 cycles, the pulse was too short to nucleate many cavitation events to yield radicals. There were not enough acoustic cycles to cause the transducer to ring up and reach the sufficient acoustic pressure amplitude for inertial cavitation. This was expected as the piezoelectric ceramic of the transducer had a large (>100) Q-factor. At more than 100 cycles, it may be that most of the nucleated bubbles undergo inertial collapse in the initial 100's of cycles. However after these collapses, these bubbles may become much larger in diameter due to rectified diffusion, bubble agglomeration, and coalescence owing to the extended burst duration [25]. These large bubbles tend not to inertially collapse and instead float to the surface of the liquid medium, degassing the liquid. These degassing bubbles also prevent the sound propagation by absorption and scattering of the sound, which leads to a decrease in the sound pressure amplitude and hence a spatial reduction of the active sonochemical reaction region [25].

Furthermore, there are simply fewer number of pulses at 10^3 and 10^4 cycles under a fixed period of reaction time compared to 100 cycles. If the bulk of the HO• production occurred in the first few hundred cycles, the fewer number of pulses also may be a reason for a lower net HO• yield. Some literature also suggested that the intervals between the pulses allow enough time for surfactants (*e.g.*, sodium 4-octylbenzene sulfonate (OBS) and sodium dodecylbenzenesulfonate (DBS)) to diffuse and accumulate around the cavitation bubbles surface [29,30]. However, it is unclear if this also occurs in our system considering the lifetime of HO• is short compared to the diffusion time of surfactants. Also, cavitation was spontaneous and transient. It was likely that cavitation bubbles condensed between pulses, thus there were no bubbles for chemicals to adsorb onto. Thus, at the optimal number of cycles, the pulse length was long enough for bubble nucleation and growth, but not long enough to cause degassing of the liquid. Also, the ultrasound off time may allow smaller bubbles to dissolve back into the liquid, effectively resetting the solution back to an initial state and preventing the possibility of forming larger bubbles that cause the shielding effect [25].

3.4. HO[•] production rate and SE comparisons with conventional sonochemical reactors

Once the optimal operating conditions were established, we determined the kinetics and SE for the sonochemical production of HO[•] by exposing water to ultrasound (15.1 MPa_{rms}, 100 cycles, and 9% DC) for different durations. Due to the different geometry of the transducers in the immersed horn, cup-horn reactor, and SonoCYL, the number of cycles required to reach the acoustic pressure amplitude steady state were different. Therefore, to ensure a fair comparison between different sonochemical reactors, the DC (9%) and the number of cycles (after the acoustic pressure amplitude steady state was reached) were remained constant for the reactors.

Regarding rates, the HO[•] concentration produced during ultrasound exposure was linearly proportional to the reaction time (Fig. 6 (a)). Thus, the slope of the regression line represented the HO[•] production rate. Following a similar method, we compared the HO[•] production rate from SonoCYL with other conventional reactors including the immersed horn reactor, the cup-horn reactor, and the bath reactor (Table 1). SonoCYL had at least three orders of magnitude faster HO[•] production rate compared to the immersed horn reactor and five orders of magnitude faster than the cup-horn reactor. There was no observable production of HO[•] for the bath reactor.

Similarly, Fig. 6 (b) presents the HO[•] production concentration resulting from different input electrical energy for different reactor types. Here we used the electrical energy to drive the reactor as the metric for energy in the SE calculation, which enabled the comparison of different devices unrestricted by the reactor configuration [31]. Further discussion regarding the comparison between SE calculation using electrical energy and calorimetric energy is mentioned in SI Section 12.

The results show that the horn reactor used here had a low maximum drive power (inset of Fig. 6 (b)). Thus, the amount of energy deposited was limited to the reaction time. Regardless, there was a linear relationship between drive energy and concentration of HO[•] for all reactors, and thus the slope of the line represented the SE. The SE values of the four sonochemical reactors are presented on Table 1. The SonoCYL had a SE twice that of the immersed horn reactor and nearly four orders of

Table 1

The table shows the HO[•] production rate and SE for the four sonochemical reactors using Res-DHB.

Reactor	Rate/ $\mu\text{M}_{\text{HO}^\bullet} \text{ min}^{-1}$	SE/ $\mu\text{M}_{\text{HO}^\bullet} \text{ Whr}^{-1}$
SonoCYL	159	273
Horn	0.46	107
Cup-Horn	0.0058	0.086
Bath	0	0

magnitude greater than the cup-horn reactor. The bath reactor did not produce any observable HO[•] yield. We observed the same trends of HO[•] production rate and SE for the four sonochemical reactors using terephthalic acid (TA), a conventional HO[•] probe (SI Section 13). This shows the better HO[•] production rate and SE from SonoCYL were irrespective of the HO[•] probe used.

Our results suggest that the reactor design may be an important factor to consider enhancing the HO[•] production rate and efficacy. Indeed, much of the literature suggests that the optimal range for sonochemistry is around 300 to 500 kHz [32]. Yet, it may be the case that reactor design may greatly affect the sonochemical efficiency. Indeed, many previous reports using similar reactor designs (*i.e.*, unfocused continuous wave ultrasound) have an optimal frequency for sonochemistry between 300 and 500 kHz. However, we show that 1 MHz SonoCYL was more efficient than the 583 kHz cup-horn setup. Similarly, the 35 kHz ultrasonic bath showed no observable sonochemistry whereas the 40 kHz immersed horn had an observable effect despite their similar driving frequencies. These results indicate the importance of the design of the reactor. Effectively, we were able to overcome limitations in dispersed acoustic energy found in conventional sonochemical reactors and reduce reaction times (higher HO[•] production rate) and produce HO[•] more efficiently.

Furthermore, SonoCYL's experimental results were highly reproducible. Acoustic inertial cavitation is a stochastic process that is difficult to control in nature, limiting the industrial scale up of sonochemical reactions. Moreover, the acoustic pressure is spatially dependent, making it crucial to control the position of the reaction vessel with respect to the liquid medium (volume and height) and transducer location [33,34].

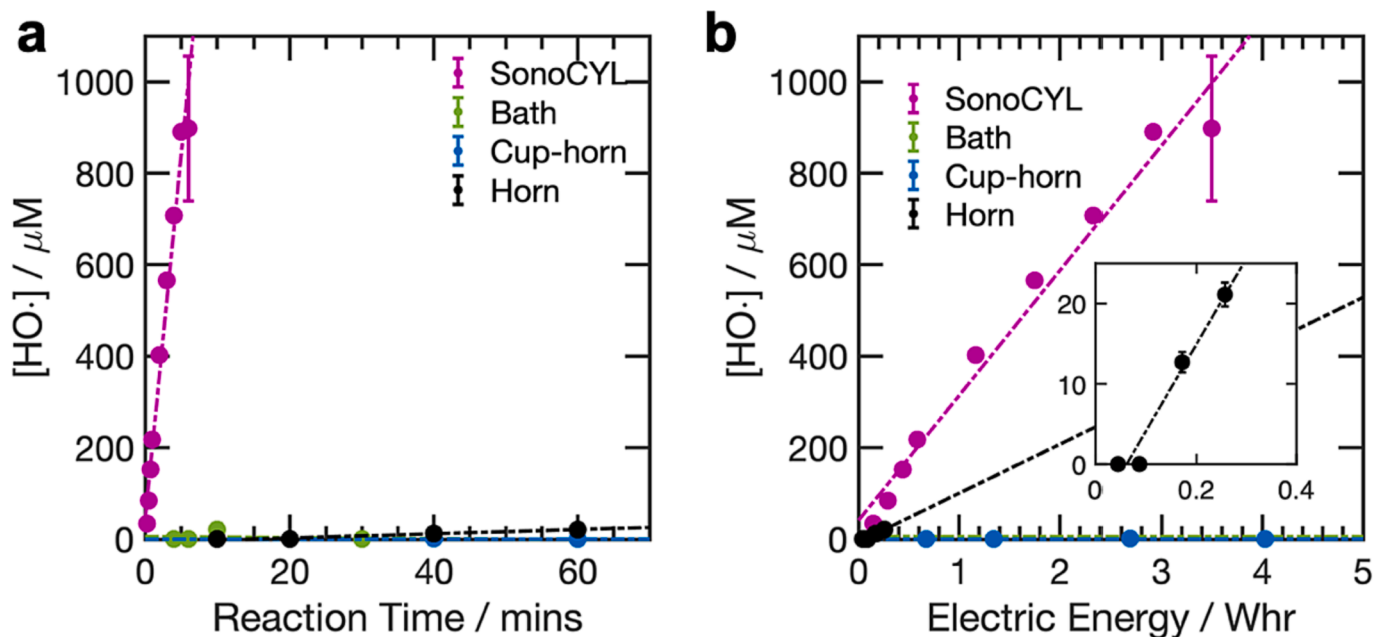


Fig. 6. (a) The HO[•] concentration vs reaction time for the four sonochemical reactors using Res-DHB: SonoCYL (1 MHz), immersed horn reactor (40 kHz), cup-horn reactor (583 kHz), and bath reactor (35 kHz) all at 9% DC. The slope of the linear regression represents the HO[•] production rate in the reaction. (b) The HO[•] concentration vs the input electrical energy for the four sonochemical reactors using Res-DHB. The slope of the linear regression represents the SE (HO[•] production per unit energy). Each value is the average of three trials and the error bars indicate the standard deviations.

Rochebrochard *et al.* demonstrated that the SE had a 9-fold difference depending on the liquid height in their cup-horn system. Similarly, Asakura *et al.* has shown the 7-fold variation in SE values with different liquid height their cup-horn system. Thus, one needs to take great care of the precise location of the reaction sample in the reactor to obtain reproducible data, which is difficult to achieve in practice with conventional sonochemical reactors. With the SonoCYL, we can accurately control the acoustic conditions within the reaction vessel resulting in highly reproducible results.

3.5. SE comparison between literature

We compared the SE of the SonoCYL with the recent sonochemical reactors in literature vs different operating frequencies (SI Table S14). The data was categorised by different sonochemical reactors (colours), power determination methods (face fill), and dosimetry methods (marker shapes) in Fig. 7.

There was no obvious trend for the SE shown in Fig. 7. It demonstrated that SE are affected by various factors including the input energy determination, the type of HO• probe, and the sonochemical reactor design. For example, the horn at 40 kHz using Res-DHB (black, circle) had a higher SE than other reactors. This may be attributed to the high sensitivity of Res-DHB compared to other dosimetry methods. Moreover, we used both the input electrical energy into the reactor (SI Figure S8) and a non-linear calorimetric method (see SI Figure S5.3) to compare the SonoCYL performance to other literature. The results showed that the SonoCYL (in purple) had a larger SE compared to other reactors at the same frequency (1 MHz) and reactors that operate at all other reported frequencies, regardless of the input energy calculation being based on electrical energy (filled, purple) or calorimetric energy (unfilled, purple). This suggests that SonoCYL is a more efficient sonochemical reactor than other conventional reactors in the literature.

Finally, Fig. 7 emphasises the lack of consensus on the way to determine SE. We believe it is important for the sonochemistry community to reach to a standard protocol to determine the SE as well as clearly report the method to determine SE for easier comparisons

between literature. This will help foster the development of sonochemical reactor design and the general field of sonochemistry in the future.

4. Conclusions

A novel sonochemical reactor (SonoCYL) using cylindrically converging acoustic waves was designed and characterised. The converging wave produced a focal volume of $\sim 1.16 \mu\text{L}$ focused on the centre of the reaction vessel. HO• yield and therefore SE were measured at varying operating conditions. SE increased with increasing acoustic pressure amplitudes but appeared to have optimal operating acoustic pressure (15.1 MPa_{rms}) and acoustic cycles (100 cycles). The HO• production rate and SE of SonoCYL was compared to conventional sonochemical reactors (an ultrasonic bath, immersed horn reactor, and cup-horn reactor). The HO• production rate was found to be at least 2 magnitude higher and the SE was at least 2 times higher compared to conventional sonochemical reactors. The same trends were observed with using TA dosimetry method. The result was likely due to both the design of SonoCYL and the optimal operating conditions. We hope that the design of SonoCYL may inspire next generation sonochemical reactor designs and lead to industrial scale-up.

CRediT authorship contribution statement

Cherie C.Y. Wong: Investigation, Visualization, Writing – original draft. **Jason L. Raymond:** Conceptualization, Methodology, Writing – review & editing. **Lillian N. Usadi:** Investigation, Visualization, Writing – review & editing. **Zhiyuan Zong:** Investigation, Writing – review & editing. **Stephanie C. Walton:** Investigation, Writing – review & editing. **Adam C. Sedgwick:** Investigation, Methodology, Writing – review & editing. **James Kwan:** Conceptualization, Writing – review & editing, Funding acquisition, Supervision.

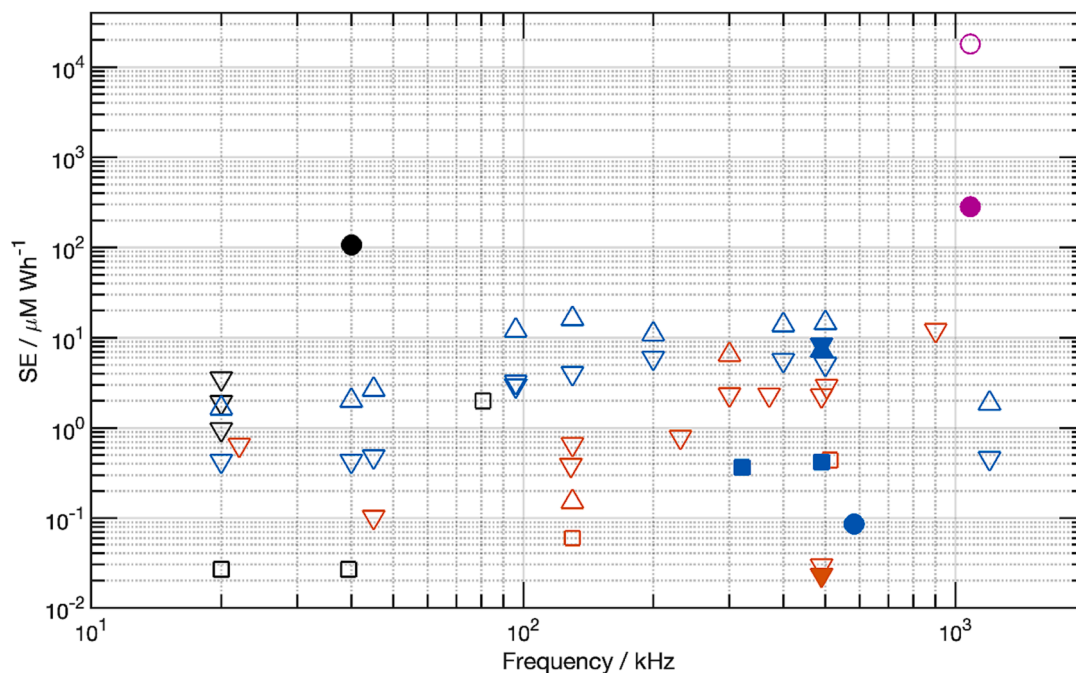


Fig. 7. SE (HO• concentration production per unit energy) vs the operating frequency of the sonochemical reactor. **Colours:** Purple – SonoCYL; Orange – Cup-horn (direct ultrasonic irradiation from the transducer to the reactant solution); Blue – Cup-horn (indirect ultrasonic irradiation from the transducer to the reactant solution); Black – Horn. **Face fill:** Filled – Drive electrical power; Unfilled – Calorimetry. **Marker shapes:** Circle (●) – Res-DHB; Upside down triangle (▼) – Weissler reaction; Triangle (▲) – Fricke reaction; Square (■) – terephthalic acid.

Declaration of Competing Interest

The authors declare that they have no known competing financial interests or personal relationships that could have appeared to influence the work reported in this paper.

Acknowledgements

C. C. Y. W. thanks the Department of Engineering Science (University of Oxford) and Balliol College (University of Oxford) for their support through the DTP Scholarship and the Dervouguilla Scholarship, respectively. L. N. U. thanks the Rhodes Trust for their support through the Rhodes Scholarship. A. C. S. would like to thank the Glasstone Research fellowship (University of Oxford) and Jesus College, Oxford for support as Junior Research Fellow.

Appendix A. Supplementary data

Supplementary data to this article can be found online at <https://doi.org/10.1016/j.ultsonch.2023.106559>.

References

- [1] K.S. Suslick, S.J. Doktycz, E.B. Flint, On the origin of sonoluminescence and sonochemistry, *Ultrasonics* 28 (1990) 280–290.
- [2] M.H. Islam, O.S. Burheim, B.G. Pollet, Sonochemical and sonoelectrochemical production of hydrogen, *Ultrason. Sonochem.* 51 (2019) 533–555.
- [3] R.S. Silva, D.L.H. Maia, F.A.N. Fernandes, Production of tung oil epoxy resin using low frequency high power ultrasound, *Ultrason. Sonochem.* 79 (2021), 105765.
- [4] S.M. Dubey, V.L. Gole, P.R. Gogate, Cavitation assisted synthesis of fatty acid methyl esters from sustainable feedstock in presence of heterogeneous catalyst using two step process, *Ultrason. Sonochem.* 23 (2015) 165–173.
- [5] T.S.H. Leong, S. Manickam, G.J. Martin, W. Li, M. Ashokkumar, *Ultrasonic Production Of Nano-Emulsions For Bioactive Delivery In Drug And Food Applications*, Springer, 2018.
- [6] T. Leighton, *The Acoustic Bubble*, Academic press, 2012.
- [7] P. Greillier, C. Bawiec, F. Bessière, C. Lafon, Therapeutic ultrasound for the heart: state of the Art, *IRBM* 39 (4) (2018) 227–235.
- [8] J.R. BlakePerutz, K.S. Suslick, Y. Didenko, M.M. Fang, T. Hyeon, K.J. Kolbeck, W. B. McNamara, M.M. Mdleleni, M. Wong, Acoustic cavitation and its chemical consequences, *Philos. Trans. Royal Soc. London Series A: Math. Phys. Eng. Sci.* 357 (1751) (1999) 335–353.
- [9] E.A. Serna-Galvis, J. Porras, R.A. Torres-Palma, A critical review on the sonochemical degradation of organic pollutants in urine, seawater, and mineral water, *Ultrason. Sonochem.* 82 (2022), 105861.
- [10] D. Meroni, R. Djellabi, M. Ashokkumar, C.L. Bianchi, D.C. Boffito, Sonoprocessing: from concepts to large-scale reactors, *Chem. Rev.* (2021).
- [11] C.C.Y. Wong, L.-L. Sun, M.-J. Liu, E. Stride, J.L. Raymond, H.-H. Han, J. Kwan, A. C. Sedgwick, Fluorescence-based chemical tools for monitoring ultrasound-induced hydroxyl radical production in aqueous solution and in cells, *Chem. Commun.* 59 (2023) 4328–4331.
- [12] D.B. Rajamma, S. Anandan, N.S.M. Yusof, B.G. Pollet, M. Ashokkumar, Sonochemical dosimetry: A comparative study of Weissler, Fricke and terephthalic acid methods, *Ultrason. Sonochem.* 72 (2021) 105413.
- [13] K.R. Morison, C.A. Hutchinson, Limitations of the Weissler reaction as a model reaction for measuring the efficiency of hydrodynamic cavitation, *Ultrason. Sonochem.* 16 (2009) 176–183.
- [14] D.A. Palmer, R. Ramette, R. Mesmer, Triiodide ion formation equilibrium and activity coefficients in aqueous solution, *J. Solution Chem.* 13 (1984) 673–683.
- [15] K. Matuszek, E. Pankalla, A. Grymel, P. Latos, A. Chrobok, Studies on the solubility of terephthalic acid in ionic liquids, *Molecules* 25 (1) (2019) 80.
- [16] G. Mark, A. Tauber, R. Laupert, H.-P. Schuchmann, D. Schulz, A. Mues, C. von Sonntag, OH-radical formation by ultrasound in aqueous solution – Part II: Terephthalate and Fricke dosimetry and the influence of various conditions on the sonolytic yield, *Ultrason. Sonochem.* 5 (1998) 41–52.
- [17] J. Jing Kwan, S. Bhatnagar, Ultrasound-enhanced transdermal drug delivery, imaging technologies and transdermal delivery in skin disorders, (2019) 271–289.
- [18] R. Toegel, B. Gompf, R. Pecha, D. Lohse, Does water vapor prevent upscaling sonoluminescence? *Phys. Rev. Lett.* 85 (2000) 3165–3168.
- [19] K. Weninger, C. Camara, S. Putterman, Observation of bubble dynamics within luminescent cavitation clouds: Sonoluminescence at the nano-scale, *Phys. Rev. E* 63 (2000), 016310.
- [20] K. Yasui, T. Tuziuti, T. Kozuka, A. Towata, Y. Iida, Relationship between the bubble temperature and main oxidant created inside an air bubble under ultrasound, *J. Chem. Phys.* 127 (2007).
- [21] K. Yasui, Influence of ultrasonic frequency on multibubble sonoluminescence, *J. Acoust. Soc. Am.* 112 (2002) 1405–1413.
- [22] X. Su, U.S. Jonnalagadda, L.D. Bharatula, J.J. Kwan, Unsupported gold nanocones as sonocatalytic agents with enhanced catalytic properties, *Ultrason. Sonochem.* 79 (2021), 105753.
- [23] C. Lafon, D. Moore, M.D. Eames, J. Snell, R.A. Drainville, F. Padilla, Evaluation of Pseudorandom sonications for reducing cavitation with a clinical neurosurgery HIFU device, *IEEE Trans. Ultras. Ferroelect. Freq. Control* 68 (2020) 1224–1233.
- [24] T. Li, H. Chen, T. Khokhlova, Y.-N. Wang, W. Kreider, X. He, J.H. Hwang, Passive cavitation detection during pulsed HIFU exposures of ex vivo tissues and in vivo mouse pancreatic tumors, *Ultrason. Med. Biol.* 40 (2014) 1523–1534.
- [25] T. Tuziuti, K. Yasui, J. Lee, T. Kozuka, A. Towata, Y. Iida, Mechanism of enhancement of sonochemical-reaction efficiency by pulsed ultrasound, *Chem. A Eur. J.* 112 (2008) 4875–4878.
- [26] D.M. Deojay, J.Z. Sostaric, L.K. Weavers, Exploring the effects of pulsed ultrasound at 205 and 616kHz on the sonochemical degradation of octylbenzene sulfonate, *Ultrason. Sonochem.* 18 (2011) 801–809.
- [27] R.A. Al-Juboori, T. Yusaf, L. Bowtell, Energy conversion efficiency of pulsed ultrasound, *Energy Procedia* 75 (2015) 1560–1568.
- [28] Z. Pan, W. Qu, H. Ma, G.G. Atungulu, T.H. McHugh, Continuous and pulsed ultrasound-assisted extractions of antioxidants from pomegranate peel, *Ultrason. Sonochem.* 18 (2011) 1249–1257.
- [29] L. Yang, J.F. Rathman, L.K. Weavers, Degradation of alkylbenzene sulfonate surfactants by pulsed ultrasound, *J. Phys. Chem. B* 109 (2005) 16203–16209.
- [30] D.J. Casadonte, M. Flores, C. Petrier, Enhancing sonochemical activity in aqueous media using power-modulated pulsed ultrasound: an initial study, *Ultrason. Sonochem.* 12 (3) (2005) 147–152.
- [31] J.-M. Löning, C. Horst, U. Hoffmann, Investigations on the energy conversion in sonochemical processes, *Ultrason. Sonochem.* 9 (3) (2002) 169–179.
- [32] S. Koda, T. Kimura, T. Kondo, H. Mitome, A standard method to calibrate sonochemical efficiency of an individual reaction system, *Ultrason. Sonochem.* 10 (3) (2003) 149–156.
- [33] S. de La Rochebrochard, J. Suptil, J.-F. Blais, E. Naffrechoux, Sonochemical efficiency dependence on liquid height and frequency in an improved sonochemical reactor, *Ultrason. Sonochem.* 19 (2) (2012) 280–285.
- [34] Y. Asakura, T. Nishida, T. Matsuoka, S. Koda, Effects of ultrasonic frequency and liquid height on sonochemical efficiency of large-scale sonochemical reactors, *Ultrason. Sonochem.* 15 (3) (2008) 244–250.